Noname manuscript No.
(will be inserted by the editor)

A Deep Non-Negative Matrix Factorization Neural Network

Jennifer Flenner · Blake Hunter

1 Abstract

Recently, deep neural network algorithms have emerged as one of the most successful machine learning strategies, obtaining state of the art results for speech recognition, computer vision, and classification of large data sets. Their success is due to advancement in computing power, availability of massive amounts of data and the development of new computational techniques. Some of the drawbacks to these deep neural networks are that they often require massive amounts of observed data, their feature representations are hard to interpret and they are not well mathematically understood when they will work, and why. Other strategies for data representation and feature extraction, such as topic modeling based strategies, have also recently progressed. Topic models, such as NMF, combine data modeling with optimization to learn interpretable and consistent feature structures in data. Previously criticized for their computational complexity, it is now possible to quickly perform topic modeling on massive streaming data sets. We introduce a deep non-negative matrix factorization framework capable of producing interpretable hierarchical classification of many types of data. Our proposed framework shows that it is possible to combine the interpretability and predictability of topic modeling learned representations with some of the power and accuracy of deep neural networks. Furthermore, we uncover a new connection between sparse matrix representations and deep learning models by combining multiple layers of NMF with a non-linear activation function and pooling, optimized by backpropagation.

2 Introduction

Deep neural network learns an input-output network composed of multiple layers of representations [Krizhevsky et al., 2012] based on massive amounts of training data. In particular, deep convo-

J. Flenner
Institute of Mathematical Sciences, Claremont Graduate University, Claremont, CA 91711, USA
E-mail: jennifer.flenner@cgu.edu

B. Hunter
Mathematical Sciences Department, Claremont McKenna College, Claremont, CA 91711, USA
E-mail: bhunter@cmc.edu

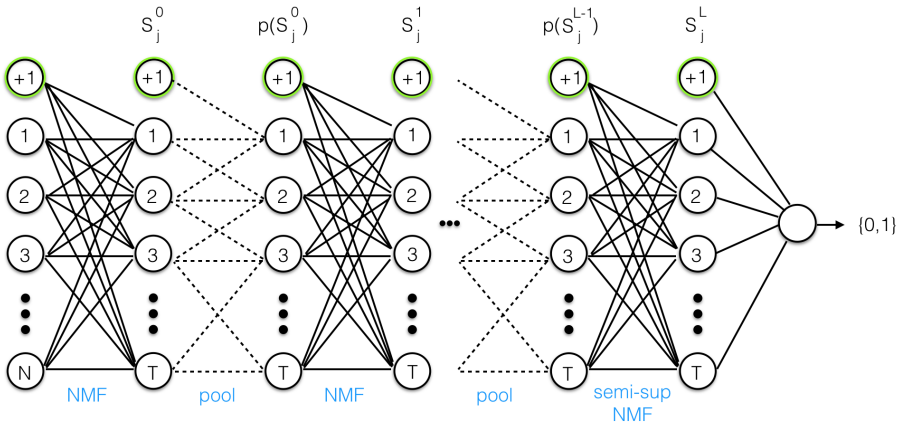

Fig. 1: A graphical representation of the deep topic model.

lutional neural networks are the current industry leaders in image classification, speech recognition, and classification of many other large data sets. They have obtained state of the art results for classification, even surpassing human level performance [He et al., 2015b, Amodei et al., 2015, Le Roux et al., 2015, Boureau et al., 2010, LeCun et al., 2015, Gan et al., 2015, Flenner et al., 2015]. One of the major drawbacks of the deep learning approach is that the models are not well understood mathematically. For example, there are no known convergence criteria, the accuracy is unpredictable, and little is known a priori where or why they fail, at times misclassifying data with high confidence [Nguyen et al., 2015]. However, other strategies for data representation and feature extraction, such as topic modeling based strategies [Blei, 2012, Lee and Seung, 1999], are well understood [Cichoki et al., 2009, Rajabi and Ghassemian, 2015]. Topic models combine data modeling with optimization to learn interpretable and consistent features in data [Blei and Lafferty, 2009, Hoyer, 2004].

We combine a deep architecture, containing multiple layers, pooling, nonlinearities, and backpropagation, with the interpretability of topic modeling. Figure 1 shows a graphical representation of the alternating generative model and pooling layers of deep non-negative matrix factorization (deep NMF). These alternating layers and the last semi-supervised linear classifier layer are learned using backpropagation. This proposed deep NMF is capable of producing reliable, interpretable, and predictable hierarchical classification of text, audio and image data. Like NMF our proposed deep models learn through optimizing an energy function. We demonstrate that it is natural to leverage pooling and backpropagation from deep neural networks and combine them with NMF based representations. First we propose a multilayered NMF that provides a hierarchical topic model, as seen in Figure 4 and 3 . Secondly, we use this multilayered NMF, combined with pooling, as a model for a deep neural network, as seen in Figure 1. This allows us to create a single efficient numerical algorithm that optimizes a deep multilayered NMF model that maintains the generative interpretable nature of NMF at the top layers while simultaneously obtaining state of the art classification accuracy of deep neural networks. Furthermore, we empirically show that connecting multiple layers with a non-linear function, followed by backpropagation, promotes sparsity.

2.1 Non-negative Matrix Factorization

A linear algebra based topic modeling technique called non-negative matrix factorization (NMF). This method was popularized by Lee and Seung through a series of algorithms [Lee and Seung, 1999], [Leen et al., 2001], [Lee et al., 2010] that can be easily implemented. Given a data matrix X such that $X_{ij} \geq 0$, non-negative matrix factorization finds a data representation by solving the optimization problem

$$\min_{A,S} ||X - AS||_F, \quad \text{such that } A_{ij} \geq 0,\ S_{ij} \geq 0, \tag{1}$$

where $|| \cdot ||_F$ is the Frobenius norm. This optimization provides a generative model of the data through linear non-negative constraints, data matrix X into a basis matrix A and corresponding coefficient matrix S.

Minimization in each variable A, S separately is a convex problem, but the joint minimization of both variables is highly non-convex [Cichoki et al., 2009]. Many NMF algorithms can get stuck in local minima, therefore, the algorithm's success can depend on initialization. This problem can often be overcome by providing several random initializations and keeping the factorization that maximizes some performance criteria.

Due to its speed and simplicity, we use the multiplicative update equations, originally derived by Lee and Seung [Lee and Seung, 1999], to optimize Equation 1. Let $A \odot B$ represent component wise multiplication, i.e. $(A \odot B)_{ij} = A_{ij}B_{ij}$ and let division be defined component wise for non-zero entries; the update equations are given by

$$A \leftarrow A \odot \frac{XS^T}{ASS^T}, S \leftarrow S \odot \frac{A^T X}{A^T AS}. \tag{2}$$

2.2 Deep Learning and Deep Neural Networks

Deep learning and deep neural networks are a rebirth of artificial networks from the 80's inspired by biological nervous systems [LeCun et al., 2015]. The first generation of learning algorithms fell out of favor due to a performance plateau when applied to increasingly large data sets. The current iteration of fully supervised learning algorithms are producing state of the art results for voice recognition, machine translation, and image classification problems [Deng et al., 2013, Bengio, 2013, Deng, 2014, Krizhevsky et al., 2012] because their performance continues to improve as the training data set size increases. The modern rendition of these algorithms are able to scale with the data. The two most powerful changes to modeling and computational techniques have been the introduction of multiple hidden layers and backpropagation.

Previously there have been attempts to combine supervised deep neural networks with unsupervised representations. One common way of combining these is using autoencoders. Autoencoders are a class of self-supervised neural networks that learn a data representation which approximates it's own input. Initially, autoencoders were once seen as a promising way to initialize deep neural networks, however, single layer neural networks have failed to produce as high of an accuracy as random initializations [He et al., 2015a].

Given a set of samples x_n, deep NN sometimes define the autoencoder as an unsupervised generative algorithm that solves the optimization problem

$$\min_W \sum_{n=1}^{N} ||x_n - f(x_n, W)||,$$

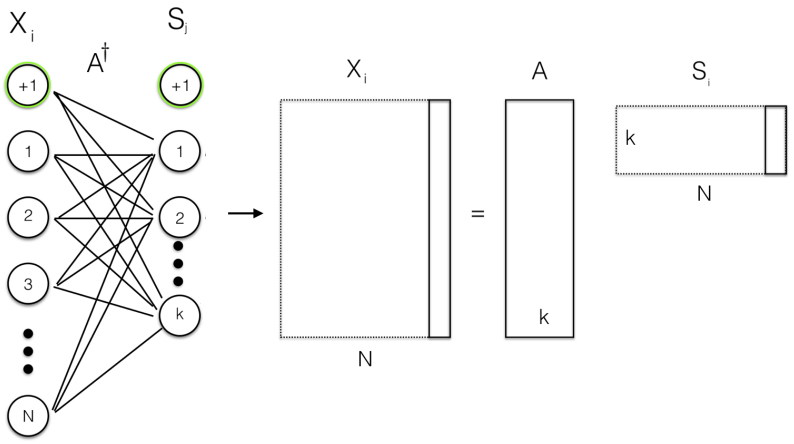

Fig. 2: On the left are the weights $A\dagger$ of a single layer neural network and on the right is an approximate matrix representation from the NMF factorization $X = AS$.

for some norm $||\cdot||$ and some single layer neural network $f(x, W)$ with parameters W. Let s_n be the column of S corresponding to the n^{th} column of X, then the autoencoder's per document optimization energy functional can be written as

$$||x_n - f(x_n, W)|| = ||x_n - As_n|| = ||x_n - AA_{auto}x_n||. \tag{3}$$

The goal of an autoencoder is to learn the operators A and A_{auto} that minimizes (3). Let $A^\dagger$ be the More-Penrose pseudo-inverse, $(A^\top A)^{-1}A^\top$ of A, then using NMF to factor $X = AS$ gives $A^\dagger X = S$ and the optimal A_{auto} is $A^\dagger$.

In order to learn more interesting features than the linear model given above, it is typical for a neural network to include a nonlinear activation function $g(x)$. Some common choices of are the softplus function [Glorot et al., 2011], the sigmoid function [Cybenko, 1989, Hornik et al., 1989], and the rectifier [Nair and Hinton, 2010, LeCun et al., 2015]. The *ReLu* rectifier activation function given by

$$g(z) = max(0, z),$$

is a commonly used activation function in deep learning ana the most applicable for non-negative matrix factorization since it is approximated by requiring all dictionary weights to be non-negative. More precisely, if we change the optimization to

$$||x_n - As_n|| \rightarrow ||x_n - Ag(s_n)||,$$

then we have included a non-negative constraint on the weights $s_n = A^\dagger x_n$. However, this is still not equivalent to NMF since A is not constrained to have non-negative elements. This is a very important distinction because the columns of A are the basis vectors that give physical meaning to the NMF generative model. Figure 2 shows an analogy between the weights $A\dagger$ of a single layer neural network and the More-Penrose pseudo-inverse of A from the NMF factorization $X = AS$.

Self-supervised algorithms, such as the autoencoders, often do not learn interesting features. For example, there is nothing preventing an autoencoder from learning the identity function. Along these lines, a stacked autoencoder, capable of learning several layers of a function, was developed. However, the set of stacked autoencoders tended to learn a lossy reconstruction which was either PCA or a close approximation [Baldi and Hornik, 1989, Chicco et al., 2014]. The lossy reconstructed data learned by autoencoders was used as a pre-training technique for deep networks.

Currently, one of the most successful methods for image classification is the Imagenet contest winner, a deep convolutional neural network [Russakovsky et al., 2015a, Russakovsky et al., 2015b]. Deep convolutional neural networks learn a data representation at each layer. Each of the deep convolutional layers has a set of parameters, weights and biases, that are learned through labeling and a fixed pooling layer that does not learn any parameters. The goal is to determine the parameters that provide good classification performance for new, unseen, data samples. The purpose is not only to find repeatable representative patterns in the data, but also to perform directed tasks on a large data set, such as classification, object recognition, and denoising [Wang, 2016, LeCun et al., 2015]. The patterns discovered by deep convolutional neural networks are designed to produce classification labels. However, these patterns, or filters, are often not interpretable or physically meaningful, and the learned coefficients are not able to accurately reconstruct the data. This is a direct result of the fact that these deep models are not required to be generative models; they are focused on learnability, not representability.

2.2.1 Limitations of standard deep Neural Networks

Deep learning algorithms constructed of hierarchical nested layers, specifically, deep convolutional neural networks [He et al., 2015b], [Russakovsky et al., 2015b], have recently lead the field in producing state of the art classification results, at times matching or exceeding human classification, for problems related to extremely large data sets. However, despite recent success, there are four main limitations to these methods.

First, regardless of all the efforts to understand why deep models produce excellent classification results, these approaches are still not well understood [Giryes et al., 2015]. Currently there is no coherent framework for understanding the functionality of each of the layers of deep algorithms [Bruna and Mallat, 2013], which renders construction of an optimal deep neural network architecture for a specific mathematical problem to be more art than science [Szegedy et al., 2015]. If we consider the example of Figure 2, which map autoencoder deep generative models to the NMF topic model, the difficulty of a formal analysis becomes clear. The operators in the autoencoder do not have a fixed mathematical interpretation. Secondly, if the generative model requirement is removed, then the output of the network is not physically interpretable [LeCun et al., 2015]. Additionally, deep neural networks are still subject to a host of common problems such as: overfitting, generalization error, and training computation time [Bengio, 2013]. Lastly, deep neural networks only work well form massive data sets, but do not perform well, overfitting or underfitting data, on problems with limited observed training data or small data sets.

This paper makes contributions to our understanding and potential resolution of each of these four problems. First, our deep NMF addresses the issue of mathematical understanding since the operators in each layer are linear algebraic operators. The function and behavior of these operators is well understood and can be analyzed in the context of a deep architecture. Second, our deep NMF retains the generative model requirement. Deconstruction of data by NMF is a method of blind source separation. The results of this deconstruction will be physically interpretable and although

reconstruction will be lossy, we are likely to retain important features in the signal. Third, we show that although NMF learns a basis size dependent on rank restriction in the first layer, the deep NMF algorithm can shrink or grow the size of the learned basis through additional hidden layers. In addition to learning a basis dimension through hidden layers, we still have access to resize the dimension through rank restriction. Control over rank restriction reduces computation time and can be used to prevent overfitting or underfitting of the data. This is a powerful additional level of control which can be used with $L2$ regularization, $L1$ regularization and dropout methods. Finally, it is well known that NMF works well on small data sets, and in fact, it has only recently been scaled to perform well on extremely large data sets. The generative, feature preserving aspects of this model, enable it to perform well on any size data set.

3 Proposed Methods

Deep networks are compositions of different functions, or network layers, commonly referred to as hidden layers. The most successful deep network for the Imagenet data set [Russakovsky et al., 2015a], is a deep convolutional neural network, [Krizhevsky et al., 2012], which consists primarily of two different types of network layers that we reproduce in our optimization framework . [Szegedy et al., 2015, Chen et al., 2014] and [Hannun et al., 2014, Graves et al., 2013] are the industry leading methods in image classification, hyperspectral segmentation and speech recognition and all uses deep variations convolutional NN. Standard deep convolutional N.N. are made up of multiple pairs of a dictionary learning layer (typically convolutional operators) and a pooling layer [Long et al., 2015] that learn a hierarchy of linear affine operators on the data.

Consider a standard deep N.N. made up of three components,

1. Multiple "hidden" layers
   (a) a affine functional $Ax + c$ layer
   (b) non-linear activation function $g(Ax + c)$ such as ReLu
   (c) pooling layer
2. supervised classification last (outer) layer
3. optimized by backpropagation.

Theorem 1 *A standard deep N.N. defined above can be written as a multi-layered deep nonnegative matrix factorization (Deep NMF) optimization.*

Proof The multiple "hidden" layers can be written as a multi-layered matrix factorization (section 3.2) by defining affine matrix functions (**??**). The ReLu Activation function is a standard approximation of a non-negative constraint (3.2.1). The pooling operator can be a combined with a NMF model (3.2.2). The last last supervised (outer) layer can be replaced with a semi-supervised NMF layer (3.2.3). Finally our proposed deep MNF network can be optimized by backpropagation (3.4).

3.1 Deep NMF

Our deep NMF model consists of multilayered NMF combined with a pooling layer followed by backpropagation. The multilayered NMF consists of nested NMF decompositions into $\mathcal{L}$ layers. After the primary data observations are deconstructed, each subsequent data layer is acted upon by a pooling function prior to each subsequent NMF decomposition. The last, or $\mathcal{L}$, layer of multilayered

NMF is decomposed by semi-supervised NMF, instead of NMF. The semi-supervised step is used to create a label learning energy functional which softens the invertibility requirement; backpropagation acts on the energy functional to learn a better set of basis coefficients. Backpropagation on the energy functional is what is known as the learning step of the algorithm. This model will be analyzed in three parts: multilayered NMF, supervised multilayered NMF with pooling, and deep NMF with backpropagation.

3.2 Multilayered NMF

Consider the independent nested set of NMF decompositions. Let $X^{(0)}$ be the original data observations. Each column in the spectrogram is a document, the sum of all the documents is called the corpus. Let the corpus, $X^{(0)}$, be the first input. The first NMF decomposition obtains

$$X^{(0)} \approx A^{(0)} S^{(0)},$$

where $A^{(0)}$ are a set of topics, or basis vectors, and $S^{(0)}$ are the topic weights, or basis coefficients. Next the basis coefficients $S^{(0)}$ become the new input. The second layer deconstructs $S^{(0)}$ to obtain a subtopics and subtopic weights,

$$S^{(0)} \approx A^{(1)} S^{(1)}.$$

The two layer nested decomposition can be rewritten as,

$$X^{(0)} \approx A^{(0)}(A^{(1)} S^{(1)}),$$

shown graphically in Figure 4.

This process can continue in order to learn as many layers as is desired. The multilayered nested decomposition for $\mathcal{L}$ layers can be found by minimizing

$$||X^{(0)} - A^{(0)} A^{(1)} \cdots A^{(\mathcal{L})} S^{(\mathcal{L})}))||.$$

The operator defined as $A^\dagger = (A^T A)^{-1} A^T$ minimizes the ℓ_2 norm between X and AS such that $A^\dagger X = S$. This operator is called the Moore-Penrose pseudoinverse [Ben-Israel and Greville, 2003, Moore, 1920] and it is used in figure 3 for the the multilayered NMF diagram. The multilayered NMF can be calculated through the process given in algorithm 5.

Let $\mathbf{x} \in \mathbb{R}^d$ be an input data point. The dictionary layer is a set of functionals $l_k : \mathbb{R}^d \to \mathbb{R}$ such that

$$l_k(\mathbf{x}) = \mathbf{s}_k.$$

By the Riesz representation theorem, we can write the kth dictionary element $l_k(\mathbf{x}) = \langle \mathbf{a}_k^\dagger, \mathbf{x} \rangle$ for weights $\mathbf{a}_k^\dagger \in \mathbb{R}^d$. This means that each layer of a neural network can be written as a matrix multiplication, as seen in Figure 4 and 3. The output of all the linear operators is a vector $\mathbf{s} = (s_1, s_2, \ldots, s_K)^T = (\langle \mathbf{a}_1^\dagger, \mathbf{x} \rangle, \ldots, \langle \mathbf{a}_K^\dagger, \mathbf{x} \rangle)^T = A^\dagger x$. The $\mathbf{a}_k^\dagger$ vectors are the neural network analog to the non-negative dictionary $A^\dagger = (\mathbf{a}_1^\dagger, \ldots, \mathbf{a}_K^\dagger)$ in NMF.

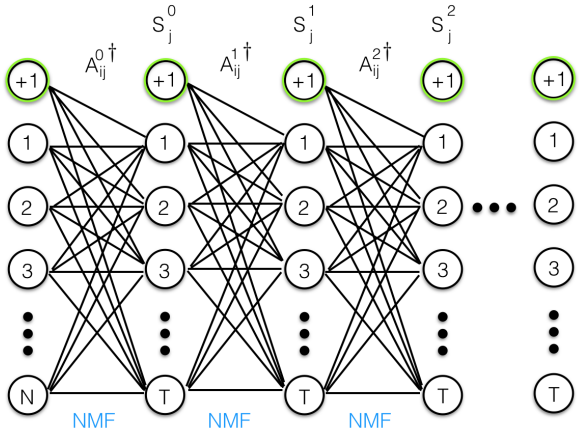

Fig. 3: The multilayered NMF model without pooling learns a hierarchical representation of the data.

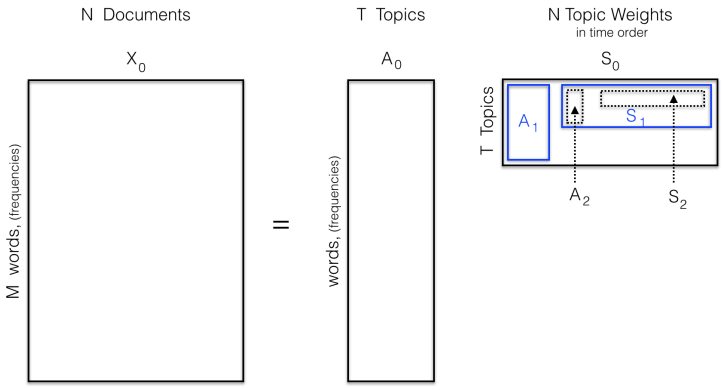

Fig. 4: The multilayered NMF model without pooling is a hierarchical representation of the data at the zeroth layer and then the weights and lower levels. This is the multilayered decomposition of the S coefficient matrices, $X^{(0)} \approx A^{(0)}(A^{(1)}(A^{(2)}S^{(2)}))$.

3.2.1 Activation Function

Neural networks often then apply an activation function $g(z)$. Some common choices are the softplus function, the sigmoid function and the rectifier. Applying the rectifier activation function, given by

$$g(z) = max(0, z),$$

can be mimicked by requiring all dictionary weights to be non-negative.

For $l < D$ the second layer of the network, the max pooling layer, is defined by the set of functions

Algorithm 1: Multilayered NMF

Data: $\mathbf{X} \in \mathbb{R}^{m \times n}$ from a collection of n documents.
The number of layers L.
The number of columns to pool across, poolsize.
Result: A nonnegative matrix decomposition at each layer l.
Initialize using forward propagation
for *l to l-1* **do**
  while *not converged* **do**

$$A^{(l)} \leftarrow A^{(l)} \odot \frac{X^{(l)}(S^{(l)})^T}{A^{(l)}S^{(l)}(S^{(l)})^T},$$

$$S^{(l)} \leftarrow S^{(l)} \odot \frac{[A^{(l)}]^T X^{(l)}}{[A^{(l)}]^T A^{(l)} S^{(l)}},$$

  end
  $X^{(l+1)} \leftarrow S^{(l)}$
  $l \leftarrow l + 1$
end

Fig. 5: The multilayered NMF forward propagation algorithm.

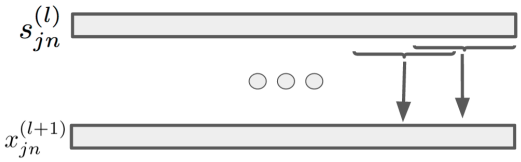

Fig. 6: Illustration of the pooling operator.

$$p_k(\mathbf{x}) = \max\{x_k \,|\, j - l \leq k \leq j + l,\, 0 \leq j \leq D\}.$$

We define $p(\mathbf{x}) = (p_1(\mathbf{x}), p_2(\mathbf{x}), \ldots, p_K(\mathbf{x}))$ as the pooling function, see Figure 6. For each row of the matrix S, the pooling operator non-linearly maps a subset of the row to one output value. The deep convolutional N.N. pooling layer can be constructed with an average pooling function [Oyallon et al., 2013] or the max pooling function. Analysis and experiments on sparse data by [Boureau et al., 2010] indicate that max pooling outperforms average pooling, so we implement max pooling as well.

A final layer is the classification function $g : \mathbb{R}^{d \times N} \to \mathbb{R}^N$. This function maps the final layer to an integer as seen in Figure 1.

A deep neural network is a composition of the network functions with a different parameter set, $A^{(l)}$, when applicable [Jia et al., 2014]. Define $f_l(\mathbf{x}) = f(\mathbf{x}, A^{(l)})$ as the convolution function

with parameter set $A^{(l)}$. The output of our neural network with $\mathcal{L}$ layers, denoted as $h(\mathbf{x})$, is the composition of functions.

Note that the output of a pooling layer, p, is the input to a dictionary learning layer f_l.

In order to optimize these parameters on the training data, [Williams and Hinton, 1986] suggests the backpropagation method. Backpropagation depends on calculating derivatives of the pooling function, but the derivative of the max function does not always exist. Where it exists, the derivative of the max function can be written as

$$\frac{\partial \max(\mathbf{x})}{\partial x_k} = \begin{cases} 1 & \text{if } \max(\mathbf{x}) = x_k, \\ 0 & \text{otherwise} \end{cases} .$$

This derivative can be used to define the derivative of $p(\mathbf{x})$ with respect to each of the components of the vector $\mathbf{x}$. A derivation of the derivative of the pooling operator will be presented after the deep NMF section.

3.2.2 Multilayered NMF with Pooling

Pooling layers are commonly found in many deep Neural networks such as [Scherer et al., 2010, Szegedy et al., 2015], but it is still not well understood why [Bruna and Mallat, 2013]. However, it is hypothesized that the purpose of a pooling step in neural networks is to reduce the spatial size of the representation to control overfitting, to create robustness to small variations and to introduce nonlinearity into the system. The most common form of pooling is to replace a neighborhood of data points with their maximum value; this is called max pooling. Inclusion of a pooling step in the deep NMF model allows us to mimic a deep neural network and investigate the impact of this operation.

We include a pooling step in our deep NMF model by placing a pooling layer after NMF decomposition in each layer. The first NMF decomposition is the original data matrix, followed by max pooling step on the weight matrix, S. The max pooling step is a window of fixed size that is moved across the data matrix columns. Every pixel in the window is replaced with the maximum pixel value found in the window; the resulting data matrix is called $p(S)$. Once the max pooling step is performed the $p(S)$ matrix is decomposed by NMF.

It is important to note that the pooling layer typically operates along the direction of a symmetry group in the data. See [Bruna and Mallat, 2013] for more information. Consider the NMF decomposition of the data

$$\mathbf{x}_n \approx A\mathbf{s}_n.$$

The pooling layer takes as input the rows of the weight matrix S_l. We use superscripts to represent row vectors of S, thus $\mathbf{s}^k \in \mathbb{R}^M$ is the k^{th} row of matrix S.

Let S be the NMF matrix from layer l. Define the rows of the data matrix X for the next layer as the pooled weights from layer $l-1$, or

$$\mathbf{x}^{k+1} = p(\mathbf{s}^k).$$

We will also use the notation $X = p(S)$ to represent the matrix where each row of the matrix is the output of the pooling operator defined above.

Algorithm 2: Supervised NMF Forward Propagation

Data: $\mathbf{X} \in \mathbb{R}^{m \times n}$ from a collection of n documents.
The number of layers L.
The number of columns to pool across, poolsize.
Result: A nonnegative matrix decomposition at each layer l.
Initialize using forward propagation
while *not converged* **do**

$$
\begin{aligned}
A^{(l)} &\leftarrow A^{(l)} \odot \frac{X^{(l)}(S^{(l)})^T}{A^{(l)}S^{(l)}(S^{(l)})^T}, \\
S^{(l)} &\leftarrow S^{(l)} \odot \frac{[A^{(l)}]^T X^{(l)}}{[A^{(l)}]^T A^{(l)} S^{(l)}}, \\
X^{(l+1)} &\leftarrow p(S^{(l)}) \\
S^{(L)} &\leftarrow S^{(L)} \odot \frac{[A^{(L)}]^T X^{(L)} + B^T Y}{[A^{(L)}]^T A^{(L)} S + B^T B S^{(L)}}, \\
B &\leftarrow B \odot \frac{Y(S^{(L)})^T}{BS^{(L)}(S^{(L)})^T}.
\end{aligned}
$$

end

Fig. 7: The supervised NMF forward propagation algorithm with pooling. This algorithm deconstructs the final input layer, $p(S^{(\mathcal{L}-1)})$, with a semi-supervised NMF step.

The last pooling layer in the algorithm is followed by supervised NMF. This is necessary because we match labels only on the last layer, as in a neural network. The zeroth layer depends on the input data, while the last $\mathcal{L}$ layer is used for classification.

This completes the forward propagation of the deep NMF model, graphically shown in Figure 1 and outlined in 7.

The equation which describes the deep NMF forward propagation with pooling is an energy functional. The energy functional exploits the NMF generative model in order to describe the error between the input data and reconstruction at each layer. The energy functional written here relies on the Frobenius norm, but it is possible to construct energy functionals using other norms. The semi-supervised Deep NMF energy functional takes the form

$$
\begin{aligned}
E(X^{(l)}, A^{(l)}, S^{(l)}, B) &= \frac{1}{2}\sum_{l=0}^{\mathcal{L}} ||W \odot (X - AS)||_F^2 + \frac{\lambda}{2}||L \odot (Y - BS^{(\mathcal{L})})||_F^2, \\
&= \frac{1}{2}||W \odot (X^{(0)} - A^{(0)}S^{(0)})||_F^2 + \frac{1}{2}\sum_{l=1}^{\mathcal{L}} ||W \odot \left(p(S^{(l-1)}) - A^{(l)}S^{(l)}\right)||_F^2 + \frac{\lambda}{2}||L \odot (Y - BS^{(\mathcal{L})})||_F^2 \\
&= \frac{1}{2}||W \odot (X^{(0)} - A^{(0)}S^{(0)})||_F^2 + \frac{1}{2}\sum_{l=0}^{\mathcal{L}-1} ||W \odot \left(p(S^{(l)}) - A^{(l+1)}S^{(l+1)}\right)||_F^2 + \frac{\lambda}{2}||L \odot (Y - BS^{(\mathcal{L})})||_F^2.
\end{aligned}
$$

3.2.3 Semi-Supervised NMF Multiplicative Update Equations

The semi-supervised NMF algorithm requires a label matrix Y. Let $Y \in \mathbb{R}^{N \times K}$ be a class matrix where for each sample n then $Y_{nk} = 1$ if $\mathbf{x}_n$ is in class k and $Y_{nk} = 0$ otherwise. Next, approximate the known label matrix Y by finding a separating hyper plane defined by a new operator B such that $||Y - BS||^2$. Finally we can introduce binary indicator matrices W_{nk} and L_{nk} to model missing data and known data labels respectively as

$$W_{ij} = \begin{cases} 1, & \text{if } \mathbf{x}_{ij} \text{ is observed} \\ 0, & \text{if } \mathbf{x}_{ij} \text{ is unobserved,} \end{cases} \quad \text{and}$$

$$[L]_{:,j} = \begin{cases} 1_k, & \text{if label } \mathbf{x}_j \text{ is known} \\ 0, & \text{otherwise.} \end{cases}$$

The NMF energy function can be rewritten as

$$E(A, B, S) = \frac{1}{2}||W \odot (X - AS)||_F^2 + \frac{\lambda}{2}||L \odot (Y - BS)||_F^2,$$

and we include the constraints $A_{ij} \geq 0$, $B_{ij} \geq 0$ and $S_{ij} \geq 0$. The term λ is used to weight the importance of the labeling. If $\lambda = 0$ then the energy functional is equivalent to the unsupervised equation, a small λ can be useful if some of the data is mislabeled, and a large λ emphasizes the labels, see [Lee et al., 2010] for more details.

3.3 Deep Network Backpropagation

The backpropagation algorithm has become the standard algorithm to train the neural networks [LeCun et al., 2012, Jia et al., 2014]. Given a set of examples $\mathbf{x}_n$ with a corresponding class label $y_n \in \mathbb{Z}$ for each sample, the backpropagation algorithm defines an energy function

$$E = \frac{1}{2} \sum_{n=1}^{N} (y_n - f(\mathbf{x}_n))^2.$$

Let W_l denote the parameters for the function f_l at the l^{th} layer of the network and ∇_{W_l} represents the gradient with respect to these parameters. Using a gradient descent to minimize the energy E updates the parameters according to the rule

$$W_l^{(n+1)} = W_l^{(n)} - \eta \nabla_{W_l} E.$$

The variable η is often called the *learning rate.* An energy is defined based on the output of the network and the parameters for the l^{th} layer. This energy is then updated through the l gradients that back-propagate from the output to the l^{th} layer, hence the name backpropagation.

3.4 Deep NMF with Backpropagation

The final algorithm adds the learning step via backpropagation which we call Deep NMF with backpropagation. This algorithm optimizes over the representations weights, or basis coefficients, in order to minimize the energy functional defined through forward propagation.

Backpropagation is a way to optimize the learning step of a deep algorithm using an energy functional based on the output of a neural network. Consider the neural networks that can written as composition of (convolutional) representation layers and pooling layers with the final layer a classification layer. The neural network can be written in the form

$$h(\mathbf{x}) = g(f(p(f(\dots f(\mathbf{x}, A^{(0)}) \dots, A^{(\mathcal{L}-1)})), A^{(\mathcal{L})}).$$

It is useful to define the output of the neural network up to layer l after the dictionary learning and pooling steps respectively as

$$\begin{aligned} d_l(\mathbf{x}) &= f(p(f(\dots f(\mathbf{x}, A^0) \dots, A^{(l-1)})), A^{(l)}), \\ q_l(\mathbf{x}) &= p(f(\dots f(\mathbf{x}, A^0) \dots, A^{(l-1)})), A^{(l)}). \end{aligned}$$

Let $z(n)$ correspond to the class of the n^{th} column. Consider the energy functional, E_{NN}, the neural network energy

$$E_{NN}(\{\mathbf{x}_n\}_{n=1}^N, z) = \frac{1}{2}\sum_{n=1}^{N}(z(n) - h(\mathbf{x}_n))^2.$$

The backpropagation algorithm learns the parameters one layer at a time and is based on gradient descent of this energy, seen in algorithm 8. There are no parameters to learn for the pooling operator.

For the deep NMF model, recall the energy functional

$$\begin{aligned} E(X^{(l)}, A^{(l)}, S^{(l)}, B) = \frac{1}{2}||W \odot (X^{(0)} - A^{(0)}S^{(0)})||_F^2 + \frac{1}{2}\sum_{l=0}^{\mathcal{L}-1}||W \odot \Big(p(S^{(l)}) - A^{(l+1)}S^{(l+1)}\Big)||_F^2 \\ + \frac{\lambda}{2}||L \odot (Y - BS^{(\mathcal{L})})||_F^2. \end{aligned}$$

Recall that $p(S^{(l)}) = X^{l+1}$, we use this substitution when calculating the gradient of the energy functional.

The gradient with respect to the $A^{(l)}$ matrix is the same as the original supervised NMF algorithm and is given by the Jacobian partial derivative of the NMF energy functional E such that

$$\begin{aligned} J_E^{A^{(l)}}(A^{(l)}) &= -\Big(W \odot (X^{(l)} - A^{(l)}S^{(l)})\Big)(S^{(l)})^T, \\ &= -(W \odot X^{(l)})(S^{(l)})^T + (W \odot A^{(l)}S^{(l)})(S^{(l)})^T. \end{aligned}$$

The Jacobian derivative with respect to $S^{(l)}$ is more difficult since the layer $l+1$ depends on $S^{(l)}$ through the pooling step. The Jacobian can be found in the appendix.

The last layer $\mathcal{L}$ will be different from the other l layers. This is because the last layer introduces the classification labeling matrices L, Y and B. The last layer of the energy functional will take the form

$$E^{(\mathcal{L})} = \frac{1}{2}||W \odot \Big(p(S^{(\mathcal{L}-1)}) - A^{(\mathcal{L})}S^{(\mathcal{L})}\Big)||_F^2 + \frac{\lambda}{2}||L \odot (Y - BS^{(\mathcal{L})})||_F^2.$$

Algorithm 3: Deep NMF with Backpropagation

Data: $\mathbf{X} \in \mathbb{R}^{m \times n}$ from a collection of n documents.
The number of layers L.
The number of columns to pool across, poolsize.
Result: A nonnegative matrix decomposition at each layer l.
Backpropagation
while *not converged* **do**

$$
\begin{aligned}
A^{(l)} &\leftarrow A^{(l)} \odot \frac{X^{(l)}(S^{(l)})^T}{A^{(l)}S^{(l)}(S^{(l)})^T}, \\
J_p(S^{(l+1)}) &\leftarrow \text{Calc Jacobian } (S^{(l+1)}) \\
S^{(l)} &\leftarrow S^{(l)} \odot \frac{[A^{(l)}]^T X^{(l)} + J_p(S^{(l+1)})A^{(l+1)}S^{(l+1)}}{[A^{(l)}]^T A^{(l)}S^{(l)} + J_p(S^{(l+1)})X^{(l+1)}}, \\
X^{(l+1)} &\leftarrow p(S^{(l)}) \\
S^{(L)} &\leftarrow S^{(L)} \odot \frac{[A^{(L)}]^T X^{(L)} + B^T Y}{[A^{(L)}]^T A^{(L)}S + B^T BS^{(L)}}, \\
B &\leftarrow B \odot \frac{Y(S^{(L)})^T}{BS^{(L)}(S^{(L)})^T}.
\end{aligned}
$$

end

Fig. 8: The deep NMF backpropagation algorithm.

The Jacobian derivative with respect to B, which only occurs in the final layer $\mathcal{L}$ is

$$
\begin{aligned}
J_E^B(B) &= \lambda\Big(L \odot (Y - BS^{(\mathcal{L})})\Big)[S^{(\mathcal{L})}]^T \\
&= \lambda\Big(L \odot Y\Big)[S^{(\mathcal{L})}]^T - \lambda\Big(L \odot BS^{(\mathcal{L})}\Big)[S^{(\mathcal{L})}]^T.
\end{aligned}
$$

It does not come as a surprise that the $\mathcal{L}$ layer update equations work out to be the same as the supervised NMF algorithm update equations. The intermediate layers $S^{(l)}$ are different. The intermediate layers do not update through labeling, but rather through the Jacobian. Given the Jacobians and following the discussion above , we obtain the multiplicative update equations for deep NMF as

$$
\begin{aligned}
A^{(l)} &\leftarrow A^{(l)} \odot \frac{[W \odot X^{(l)}](S^{(l)})^T}{[W \odot A^{(l)}S^{(l)}](S^{(l)})^T}, \\
S^{(l)} &\leftarrow S^{(l)} \odot \frac{(A^{(l)})^T\Big[W \odot X^{(l)}\Big] + \Big[W \odot A^{(l+1)}S^{(l+1)}\Big][J_p(S^{(l)})]^T}{(A^{(l)})^T\Big[W \odot A^{(l)}S^{(l)}\Big] + \Big[W \odot X^{(l+1)}\Big][J_p(S^{(l)})]^T}, \\
S^{(\mathcal{L})} &\leftarrow S^{(\mathcal{L})} \odot \frac{(A^{(\mathcal{L})})^T\Big[W \odot X^{(\mathcal{L})}\Big] + \lambda B^T\Big[L \odot Y\Big]}{(A^{(\mathcal{L})})^T\Big[W \odot A^{(\mathcal{L})}S^{(\mathcal{L})}\Big] + \lambda B^T\Big[L \odot BS^{(\mathcal{L})}\Big]}, \\
B &\leftarrow B \odot \frac{\Big[L \odot Y\Big](S^{(\mathcal{L})})^T}{\Big[L \odot BS^{(\mathcal{L})}\Big](S^{(\mathcal{L})})^T}.
\end{aligned} \tag{4}
$$

The basic properties of the deep NMF algorithm are contrasted with those of a deep convolutional neural network and single layer NMF in table 3.4.

Architecture	Convolutional Deep NN	NMF	Deep NMF
Representation	$A^\dagger X = S$	X=A S	X=A S
Activation Function	ReLu: $g(z) = max(z, 0)$	non-negative restriction	non-negative restriction
f(x,w)	$Ag(A^\dagger x_n)$	$gAgA^\dagger x_n$	$gAgA^\dagger x_n$ multilayered
loss function	$\|\|z - f(x, w)\|\|$	$\|\|X - AS\|\|$	$\sum_\ell \|\|X^{(\ell)} - A^{(\ell)}S^{(\ell)}\|\|$
Layer Model	additive network weights	-	matrix multiplication
Nonlinearity	pooling	none	pooling
Representation	hierarchical convolutions	non-negative parts model	hierarchical parts model
Layers	multilayered network	single	multilayered NMF
Optimization	backpropagation	multiplicative updates & alternating least squares	backpropagation & multiplicative updates

4 Results and Discussion

4.1 Text Data Preprocessing

The corpus was processed using the Bag of Words model. The first step was to select a fixed number of classes; these classes were used to label the known data. Then, each text document was broken into paragraphs and each paragraph was broken into a histogram of words and word frequencies. These histograms were compiled into a matrix of word frequencies representing the entire corpus, every row contains a distinct word and each column is a paragraph from a specific text document. Next, stop words, such as articles and pronouns, were removed from the corpus.Then we calculate the term frequency inverse document frequency statistic , TF-IDF [Salton et al., 1975], which is used to de-emphasized words that are common among all documents, while emphasizing words

found with high frequency in a specific document. The final step is to label the training set using the predetermined classes. In this particular case, labels were known for the entire text corpus, so we randomly selected 1% of the data from each of the classes to label as known. The resulting word frequency matrix, with 1% of the data labeled, is the input for the deep NMF algorithm.

4.2 Text Experiments

The text corpus was deconstructed by the deep NMF algorithm in a series of experiments. The NMF rank restriction was fixed to 20. The training set was created from 1% of the text corpus. The deep NMF algorithm was run for two and three layer cases for each of the pool window sizes from the set $\{0, 3, 5, 7\}$. The classification results from these experiments were compared to the result of the semi-supervised NMF, SSNMF, algorithm using identical rank restriction and training parameters.

The goal of the text data deconstruction was to correctly classify each document in one of 5 classes. In order to make sure each document can be classified, we do not want to pool across more than one document at a time. This means that we can pool across sentences or paragraphs. We decided to pool across paragraphs, with the pool stops at the end of each document. The typical document contained between 10 and 30 paragraphs. We investigated pool sizes across paragraphs of size $\{0, 3, 5, 7\}$. Topic consolidation was defined as two topics having the same nonzero word list and a distribution over words within 5° of each other. During forward propagation topic consolidation did not occur without pooling as seen in 10.

Both deep NMF and SSNMF contain a supervision layer. Recall, that the multiplicative update equations trade off between labeling by minimizing $||Y - BS||$ and data reconstruction by minimizing $||X - AS||$. In the multiplicative update equations, the B matrix is created in the last layer and is used for class labeling. Therefore, the density of the B matrix indicates the number of basis elements necessary for classification. The deep NMF algorithm found a sparser basis than NMF, SSNMF, and multilayered NMF. The only two differences between deep NMF and multilayered NMF are the pooling and backpropagation steps. Pooling and backpropagation are encouraging sparsity, as seen in figure 9.

The forward propagation algorithms, multilayered NMF, learn a set of topics through the first layer NMF decomposition. The topic list does not change until backpropagation. Consider the example of the philosophy class initially deconstructed into 6 topics in layer 1 deconstruction shown in figure 10. However, after backpropagation, a new dictionary and basis weights are learned which allow us to reconstruct the original philosophy class using only two final topics and updated weights. The philosophy class is described by 6 initial topics which are condensed into 2 new final topics after backpropagation. The topic consolidation found was consistent with the B matrix results which show that deep NMF learns the sparsest basis.

Unsupervised learning is performed by classification using clustering. One way to assess the algorithmic result is to analyze cluster purity [Handl et al., 2005]. Purity is an external evaluation method used to rate the homogeneity of clustered data. Note that while purity is related to classification, it is not classification. Specifically, it is possible for purity to be high and classification to be low, or for purity to be low and classification high. The purity results of our clustered data were very similar to the correct classification rate of that data shown in figure 11 next to the classification rates.

Finally, classification rates of SSNMF, multilayered NMF and deep NMF were compared. Our deep NMF produced higher classification rates than SSNMF or multilayered NMF. The one layer

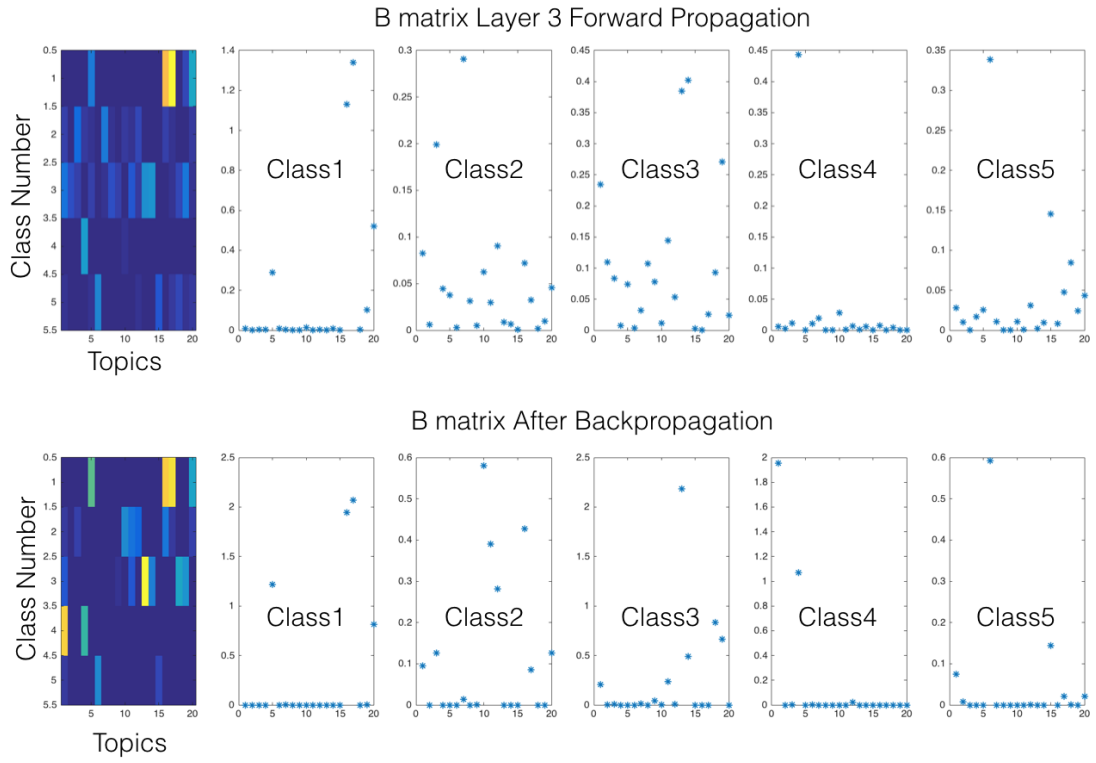

Fig. 9: The B matrix for text data is a result of the multiplicative update rules derived in Equation 4. The class 1, class 2, class 3, class 4, and class 5 graphs indicate the active topics in each class. The second row shows the B matrix after backpropagation.

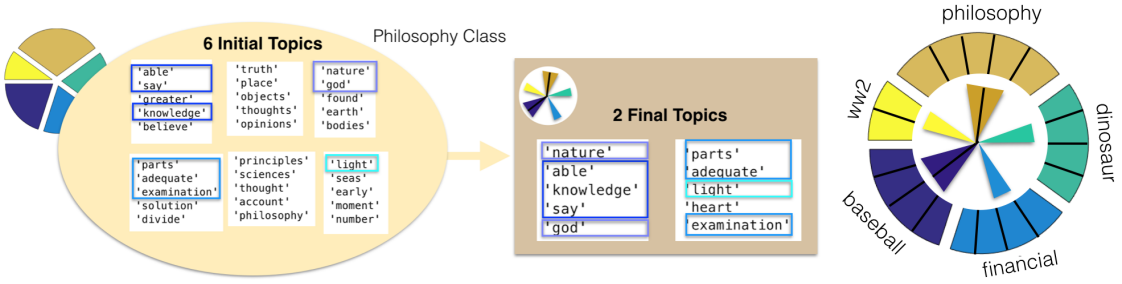

Fig. 10: The outer circle is constructed of 5 classes decomposed into an overcomplete basis of 20 initial topics. Deep NMF, after backpropagation, learns a new representation of both dictionary and weights. The inner circle shows the new restricted overcomplete basis, which reconstructs the original 5 classes into 7 learned final topics and updated weights.

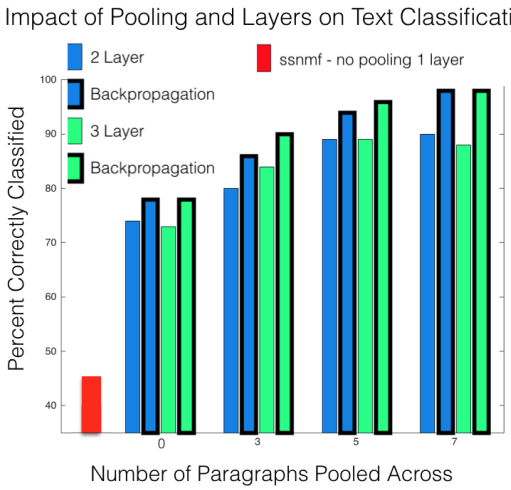

Purity Score Text Data

Pool	alg2			alg3	
	1	2	3	2	3
0	.46	.74	.76	.78	.78
3	N/A	.79	.85	.86	.90
5	N/A	.86	.83	.94	.96
7	N/A	.88	.95	.98	.98

Fig. 11: This histogram shows the impact of 2 and 3 layers with varying pool size on classification. These results were obtained by randomnly training on 1% of the data with a rank restriction of 20. These classification rates were compared with the the single layer SSNMF algorithm given the same rank and training parameters. The classification rate of single layer SSNMF was 46%.

SSNMF case obtained a classification rate of 46%. It is not possible to perform pooling or back-propagation on a one layer algorithm, so these steps were omitted. The classification results are given in figure 11.

4.3 Audio Data Preprocessing

The audio data was obtained from *The Cornell Guide To Bird Sounds Master Set For North America*, copyright 2014. The audio data consists of bird calls from three bird types: owls, woodpeckers and hummingbirds from the Cornell Master Set database. Each call was broken into 3 second segments and grouped by bird type. These calls were then converted into a spectrogram. The spectrogram is always a non-negative visual representation of the Fourier spectrum, created from an audio signal in which the rows represent frequencies and the columns are documents. Each document represents one fifty fourth of a second of a bird call. The audio data corpus consists of a concatenation of all the bird call spectrograms. We randomly selected 1% of the data from each of the three bird types to label as known. The resulting spectrogram matrix, with 1% of the data labeled, is the input for the deep NMF algorithm.

4.4 Audio Experiments

The audio corpus was deconstructed by the deep NMF algorithm in a series of experiments. The NMF rank restriction was fixed to 30. The training set was created from 1% of the audio corpus. Next, the deep NMF algorithm was run for two and three layer cases for each of the pool window sizes from the set $\{0, 25, 50, 75\}$. The classification results from these experiments were compared

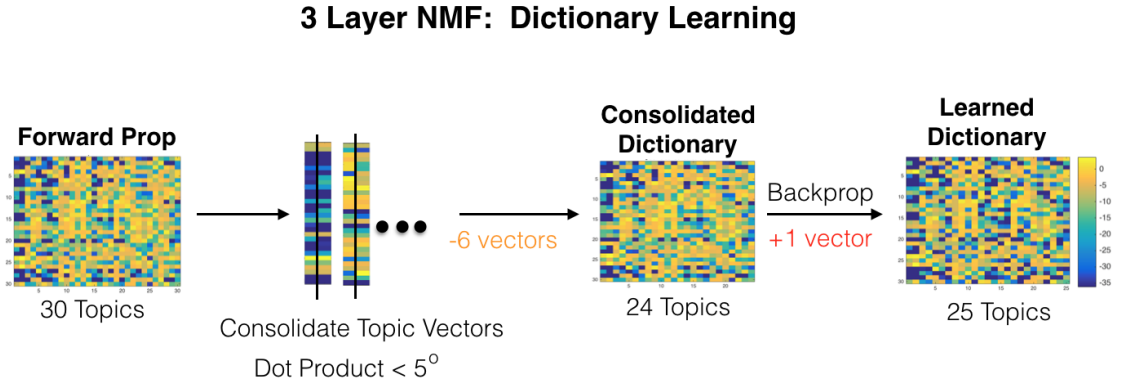

Fig. 12: The procedure for learning topics in audio data.

to the result of the semi-supervised NMF, SSNMF, algorithm using identical rank restriction and training parameters. It is important to note that the pooling layer typically operates along the direction of a symmetry group in the data. See [Bruna and Mallat, 2013] for more information. In the bird data set, the appropriate symmetry group is along the spectrogram's time axis. Consider the NMF decomposition of the data

$$\mathbf{x}_n \approx A\mathbf{s}_n.$$

Each bird call corresponds to 162 columns, or documents, in the spectrogram. For each bird we can write $S = (\mathbf{s}_1, \ldots, \mathbf{s}_M)$. Pooling along the time axis is equivalent to pooling along the columns of S, which is different than the deep neural network pooling defined above. Instead, the pooling layer takes as input the rows of the weight matrix S corresponding to the NMF spectrogram of a single bird call. We will use superscripts to represent row vectors of S, thus $\mathbf{s}^k \in \mathbb{R}^M$ is the k^{th} row of matrix S. The background, or silent periods, may be common to all bird species. Second, the background may contain other animals, which again may be common to all bird clips. The goal of pooling is to remove the nuisance variation common to all the bird classes and emphasize the unique features of each of the three bird classes. The pool stop used for the audio data was 3 seconds of a bird call. We investigated pool sizes across the spectrogram for sizes of $\{0, 25, 50, 75\}$. Topic consolidation was defined as topic vectors that are less than 5° apart.Topic consolidation did not occur without pooling as seen in 12.

The deep NMF algorithm was found to produce a sparser basis than NMF, SSNMF, and multi-layered NMF. In the audio data, it was again found that pooling and backpropagation are encouraging sparsity, as seen in figure 13. In the audio data, the topic list begins to consolidate in the forward propagation step if pooling is present. The topic list changes further after backpropagation, in which 12 shows how backpropagation can grow the number of topics. The topic consolidation was again found to be consistent with the B matrix results which show that deep NMF learns a sparser basis. The sparser basis classifies better as seen in 14.

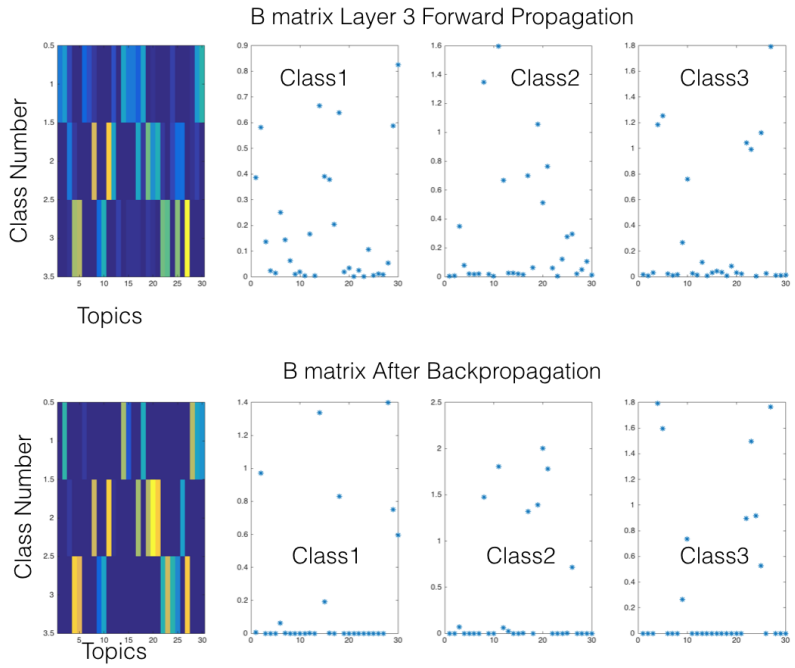

Fig. 13: The B matrix for audio data is a result of the multiplicative update rules derived in Equation 4. The class 1, class 2, and class 3 graphs indicate the active topics in each class. The second row shows the B matrix after backpropagation.

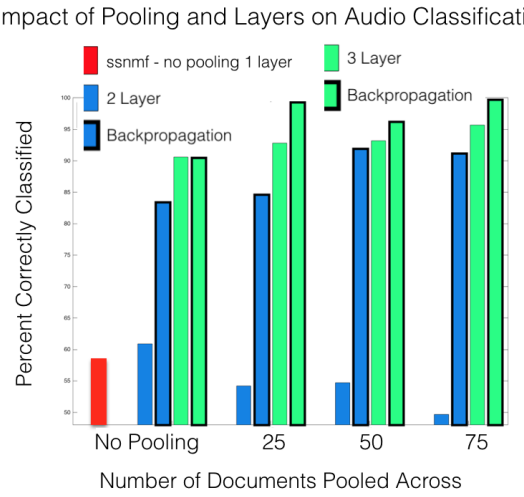

Purity Score Audio Data

Pool	alg2			alg3	
	1	2	3	2	3
0	.59	.61	.55	.54	.50
25	N/A	.83	.92	.85	.91
50	N/A	.91	.93	.93	.96
75	N/A	.90	.96	.99	.99

Fig. 14: This histogram shows the impact of 2 and 3 layers with varying pool size on classification. These results were obtained by randomnly training on 1% of the data with a rank restriction of 30. These classification rates were compared with the the single layer SSNMF algorithm given the same rank and training parameters. The classification rate of single layer SSNMF was 59%.

4.5 Insights into Neural Networks

In addition to classification, euclidean distance and angle changes within layers [Giryes et al., 2015] can be used to evaluate the learned representation found by a neural network. If we follow points through deep layers, points within the same class are expected to remain close together while points from different classes are expected to move apart. There are two criteria that must be satisfied for this premise to hold: first, the input data must lie on the surface of a sphere and the activation function is a rectified linear unit (ReLU). Although deep NMF does not use a ReLU activation function, it deconstructs a positive corpus into two non-negative matrices which provide the same non-negative initial restriction as the ReLU activation function; the outputs remain approximately on the surface of a sphere. Therefore, the input text data under the deep NMF model satisfy both conditions.

For each layer, a sample of points from a distinct class can be represented by the feature vectors $S^{(l)}$. The angular distance between these feature vectors as the representation becomes deep will change. The maximum angle of separation is 90 degrees. Let $S_a^{(l)}$ be a feature vector from class a and $S_a^{(l+1)}$ be the feature vector at the next layer. Using the polarization identity, we can define the angle between two feature vectors as

$$\theta_a^{(l)} = \operatorname{acos}\left(\frac{||S_a^{(l)} + S_a^{(l+1)}|| - ||S_a^{(l)} - S_a^{(l+1)}||}{||S_a^{(l+1)}||\,||S_a^{(l+1)}||}\right).$$

Geometrically, if the minimum angle between the input vectors and output vectors of different classes increases then the sets have an increase in separation. Let $S^{(l)}$ be a feature vector at level l. We calculate the histograms for $H(l, a)$ and $H(l + 1, a)$. If the histogram is shifted away from zero, then the class is further separated, indicating the feature vectors are from different classes. If the angle between classes shrinks, the feature vectors are from the same class. The ratio of the angle change between the last layer and the first layer can be used to determine how the points are moving through the layers. If the ratio is less than 1, the points are from the same class. If the ratio is greater than or equal to 1, then the points are from different classes. In general, the deep NMF was able to classify points from within class and between classes in the expected way, shown in figure 16.

We compare the input and output angles at each layer for deep NMF with pooling and without pooling for both the text and audio data. Figure 16 shows that without pooling the representation does not retain important within class information shown in figure 16. Pooling is adding stability as the number of layers increases; this can be seen in Figure 15.

The NMF portion of the algorithm prevents over fitting, however, it is the pooling layer which creates feature stability, and backpropagation allows us to find the features that determine the classification labels of interest. The angles between the input layer and output layer are used to find a distance. If the distance is greater than one, the points are spreading apart. If the distance is less than one the points remain close. The distance of points between two different classes is expected to grow between layers. Thus, a euclidean distance greater than one is desirable between classes, indicating that points from different classes are spread apart as seen in figure 16 and figure 17. Ideally, points from the same class remain close, or are pushed together, therefore, it is desirable to obtain a distance less than or equal to one. In figures 16 and 17 we were able to show that, in general, points from the same classes remain close, while points from different classes are spread apart. We were also able to experimentally demonstrate that in order to obtain proper distance between points the inclusion of a non-linear pooling layer is necessary.

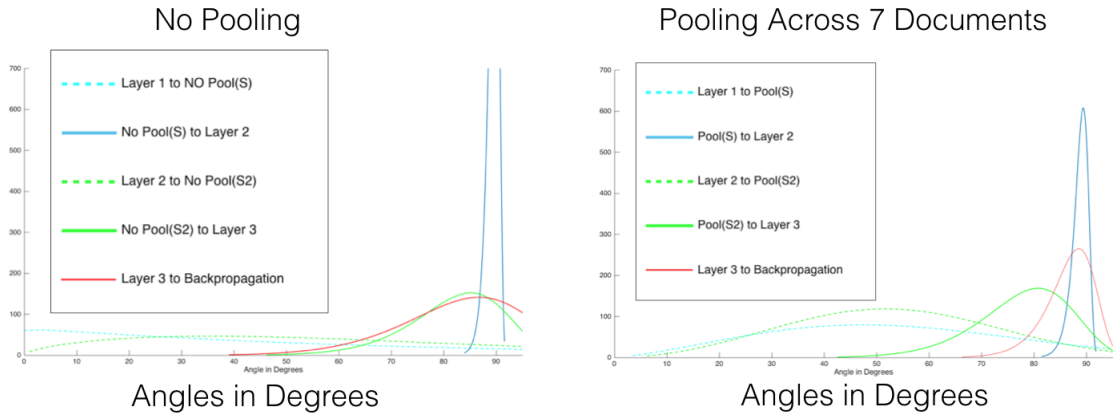

Fig. 15: Histogram of angles in the output between layers, comparing class 1 to the other classes. Note that without pooling the angle separation, through multiple layers, does not occurr.

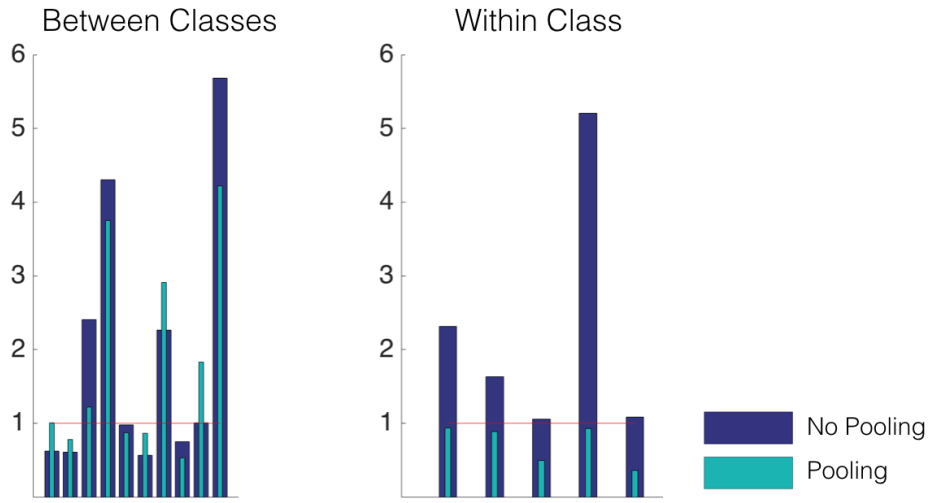

Fig. 16: The Euclidean distance for Text data points at input layer compared to output layer at the end of deep NMF. The bar graph on the left shows distance between points from different classes. The bar graph on the right shows the distance between points from the same class.

Figure 15, 16 and 17 demonstrate that extending NMF algorithms can produce the quality inter results previously only seen in deep neural networks. In particular, applying deep NMF allow points from the same class remain close while points from different classes become points become further separated as additional layers and pooling are added.

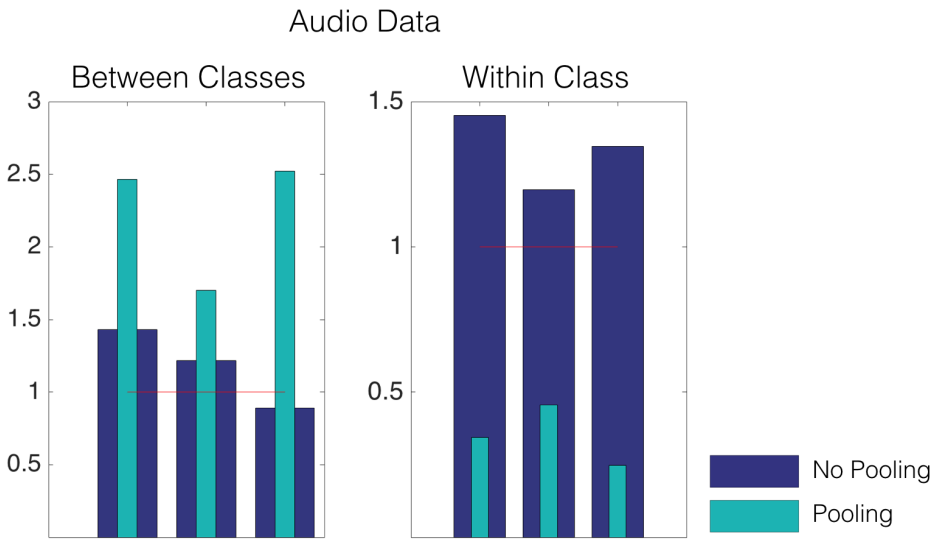

Fig. 17: The Euclidean distance for Audio data points at input layer compared to output layer at the end of deep NMF. The bar graph on the left shows distance between points from different classes. The bar graph on the right shows the distance between points from the same class.

5 Conclusion

This paper combined ideas from non-negative matrix factorization and deep convolutional neural networks, introducing a deep NMF model. We provide an efficient set of optimization update equations that combine multiplicative updates with backpropagation. We show this deep NMF framework produces interpretable hierarchical classification of text and audio data, outperforming NMF, semi-supervised NMF, and multilayered NMF. Leveraging NMF as a generative model produces a more physically interpretable output at each layer. Additionally, this generative constraint allows deep NMF to perform well on limited training data, whereas previous deep neural networks usually require massive amounts of observed data. The deep NMF model also allows us to learn the optimal rank of the data deconstruction at each layer, giving us a way to avoid overfitting or underfitting the data. Lastly, the structure of our deep NMF model provides a bridge to gain mathematical insight into general deep neural networks.

References

[Amodei et al., 2015] Amodei, D., Anubhai, R., Battenberg, E., Case, C., Casper, J., Catanzaro, B., Chen, J., Chrzanowski, M., Coates, A., Diamos, G., et al. (2015). Deep speech 2: End-to-end speech recognition in english and mandarin. *arXiv preprint arXiv:1512.02595*.

[Baldi and Hornik, 1989] Baldi, P. and Hornik, K. (1989). Neural networks and principal component analysis: Learning from examples without local minima. *Neural networks*, 2(1):53–58.

[Ben-Israel and Greville, 2003] Ben-Israel, A. and Greville, T. N. (2003). *Generalized inverses: theory and applications*, volume 15. Springer Science & Business Media.

[Bengio, 2013] Bengio, Y. (2013). Deep learning of representations: Looking forward. In *Statistical language and speech processing*, pages 1–37. Springer.

[Blei, 2012] Blei, D. M. (2012). Probabilistic topic models. *Communications of the ACM*, 55(4):77–84.

[Blei and Lafferty, 2009] Blei, D. M. and Lafferty, J. D. (2009). Topic models. *Text mining: classification, clustering, and applications*, 10(71):34.

[Boureau et al., 2010] Boureau, Y.-L., Ponce, J., and LeCun, Y. (2010). A theoretical analysis of feature pooling in visual recognition. In *Proceedings of the 27th international conference on machine learning (ICML-10)*, pages 111–118.

[Bruna and Mallat, 2013] Bruna, J. and Mallat, S. (2013). Invariant scattering convolution networks. *IEEE transactions on pattern analysis and machine intelligence*, 35(8):1872–1886.

[Chen et al., 2014] Chen, Y., Lin, Z., Zhao, X., Wang, G., and Gu, Y. (2014). Deep learning-based classification of hyperspectral data. *IEEE Journal of Selected topics in applied earth observations and remote sensing*, 7(6):2094–2107.

[Chicco et al., 2014] Chicco, D., Sadowski, P., and Baldi, P. (2014). Deep autoencoder neural networks for gene ontology annotation predictions. In *Proceedings of the 5th ACM Conference on Bioinformatics, Computational Biology, and Health Informatics*, pages 533–540. ACM.

[Cichoki et al., 2009] Cichoki, A., Zdunek, R., Phan, A., and Amari, S. (2009). Nonnegative matrix and tensor factorization.

[Cybenko, 1989] Cybenko, G. (1989). Approximation by superpositions of a sigmoidal function. *Mathematics of control, signals and systems*, 2(4):303–314.

[Deng, 2014] Deng, L. (2014). A tutorial survey of architectures, algorithms, and applications for deep learning. *APSIPA Transactions on Signal and Information Processing*, 3:e2.

[Deng et al., 2013] Deng, L., Li, J., Huang, J.-T., Yao, K., Yu, D., Seide, F., Seltzer, M., Zweig, G., He, X., Williams, J., et al. (2013). Recent advances in deep learning for speech research at microsoft. In *Acoustics, Speech and Signal Processing (ICASSP), 2013 IEEE International Conference on*, pages 8604–8608. IEEE.

[Flenner et al., 2015] Flenner, A., Culp, M., McGee, R., Flenner, J., and Garcia-Cardona, C. (2015). Learning representations for improved target identification, scene classification, and information fusion. In *SPIE Defense+ Security*, pages 94740W–94740W. International Society for Optics and Photonics.

[Gan et al., 2015] Gan, Z., Chen, C., Henao, R., Carlson, D., and Carin, L. (2015). Scalable deep poisson factor analysis for topic modeling. In *Proceedings of the 32nd International Conference on Machine Learning (ICML-15)*, pages 1823–1832.

[Giryes et al., 2015] Giryes, R., Sapiro, G., and Bronstein, A. M. (2015). Deep neural networks with random gaussian weights: A universal classification strategy? *IEEE Transactions on Signal Processing*, 64(13):3444–3457.

[Glorot et al., 2011] Glorot, X., Bordes, A., and Bengio, Y. (2011). Deep sparse rectifier neural networks. In *Aistats*, volume 15, page 275.

[Graves et al., 2013] Graves, A., Mohamed, A.-r., and Hinton, G. (2013). Speech recognition with deep recurrent neural networks. In *Acoustics, speech and signal processing (icassp), 2013 ieee international conference on*, pages 6645–6649. IEEE.

[Handl et al., 2005] Handl, J., Knowles, J., and Kell, D. B. (2005). Computational cluster validation in post-genomic data analysis. *Bioinformatics*, 21(15):3201–3212.

[Hannun et al., 2014] Hannun, A., Case, C., Casper, J., Catanzaro, B., Diamos, G., Elsen, E., Prenger, R., Satheesh, S., Sengupta, S., Coates, A., et al. (2014). Deep speech: Scaling up end-to-end speech recognition. *arXiv preprint arXiv:1412.5567*.

[He et al., 2015a] He, K., Zhang, X., Ren, S., and Sun, J. (2015a). Deep residual learning for image recognition. *arXiv preprint arXiv:1512.03385*.

[He et al., 2015b] He, K., Zhang, X., Ren, S., and Sun, J. (2015b). Delving deep into rectifiers: Surpassing human-level performance on imagenet classification. In *Proceedings of the IEEE International Conference on Computer Vision*, pages 1026–1034.

[Hornik et al., 1989] Hornik, K., Stinchcombe, M., and White, H. (1989). Multilayer feedforward networks are universal approximators. *Neural networks*, 2(5):359–366.

[Hoyer, 2004] Hoyer, P. O. (2004). Non-negative matrix factorization with sparseness constraints. *The Journal of Machine Learning Research*, 5:1457–1469.

[Jia et al., 2014] Jia, Y., Shelhamer, E., Donahue, J., Karayev, S., Long, J., Girshick, R., Guadarrama, S., and Darrell, T. (2014). Caffe: Convolutional architecture for fast feature embedding. In *Proceedings of the 22nd ACM international conference on Multimedia*, pages 675–678. ACM.

[Krizhevsky et al., 2012] Krizhevsky, A., Sutskever, I., and Hinton, G. E. (2012). Imagenet classification with deep convolutional neural networks. In *Advances in neural information processing systems*, pages 1097–1105.

[Le Roux et al., 2015] Le Roux, J., Hershey, J. R., and Weninger, F. (2015). Deep nmf for speech separation. In *Acoustics, Speech and Signal Processing (ICASSP), 2015 IEEE International Conference on*, pages 66–70. IEEE.

[LeCun et al., 2015] LeCun, Y., Bengio, Y., and Hinton, G. (2015). Deep learning. *Nature*, 521(7553):436–444.

[LeCun et al., 2012] LeCun, Y. A., Bottou, L., Orr, G. B., and Müller, K.-R. (2012). Efficient backprop. In *Neural networks: Tricks of the trade*, pages 9–48. Springer.

[Lee and Seung, 1999] Lee, D. D. and Seung, H. S. (1999). Learning the parts of objects by non-negative matrix factorization. *Nature*, 401(6755):788–791.

[Lee et al., 2010] Lee, H., Yoo, J., and Choi, S. (2010). Semi-supervised nonnegative matrix factorization. *Signal Processing Letters, IEEE*, 17(1):4–7.

[Leen et al., 2001] Leen, T. K., Dietterich, T. G., and Tresp, V. (2001). *Advances in Neural Information Processing Systems 13: Proceedings of the 2000 Conference*, volume 13. MIT Press.

[Long et al., 2015] Long, J., Shelhamer, E., and Darrell, T. (2015). Fully convolutional networks for semantic segmentation. In *Proceedings of the IEEE Conference on Computer Vision and Pattern Recognition*, pages 3431–3440.

[Moore, 1920] Moore, E. (1920). On the reciprocal of the general algebraic matrix. *Bulletin of the American Mathematical Society*, 26(9):394–395.

[Nair and Hinton, 2010] Nair, V. and Hinton, G. E. (2010). Rectified linear units improve restricted boltzmann machines. In *Proceedings of the 27th International Conference on Machine Learning (ICML-10)*, pages 807–814.

[Nguyen et al., 2015] Nguyen, A., Yosinski, J., and Clune, J. (2015). Deep neural networks are easily fooled: High confidence predictions for unrecognizable images. In *Computer Vision and Pattern Recognition (CVPR), 2015 IEEE Conference on*, pages 427–436. IEEE.

[Oyallon et al., 2013] Oyallon, E., Mallat, S., and Sifre, L. (2013). Generic deep networks with wavelet scattering. *arXiv preprint arXiv:1312.5940*.

[Rajabi and Ghassemian, 2015] Rajabi, R. and Ghassemian, H. (2015). Sparsity constrained graph regularized nmf for spectral unmixing of hyperspectral data. *Journal of the Indian Society of Remote Sensing*, 43(2):269–278.

[Russakovsky et al., 2015a] Russakovsky, O., Deng, J., Su, H., Krause, J., Satheesh, S., Ma, S., Huang, Z., Karpathy, A., Khosla, A., Bernstein, M., Berg, A. C., and Fei-Fei, L. (2015a). ImageNet Large Scale Visual Recognition Challenge. *International Journal of Computer Vision (IJCV)*, 115(3):211–252.

[Russakovsky et al., 2015b] Russakovsky, O., Deng, J., Su, H., Krause, J., Satheesh, S., Ma, S., Huang, Z., Karpathy, A., Khosla, A., Bernstein, M., et al. (2015b). Imagenet large scale visual recognition challenge. *International Journal of Computer Vision*, 115(3):211–252.

[Salton et al., 1975] Salton, G., Wong, A., and Yang, C.-S. (1975). A vector space model for automatic indexing. *Communications of the ACM*, 18(11):613–620.

[Scherer et al., 2010] Scherer, D., Müller, A., and Behnke, S. (2010). Evaluation of pooling operations in convolutional architectures for object recognition. In *International Conference on Artificial Neural Networks*, pages 92–101. Springer.

[Szegedy et al., 2015] Szegedy, C., Liu, W., Jia, Y., Sermanet, P., Reed, S., Anguelov, D., Erhan, D., Vanhoucke, V., and Rabinovich, A. (2015). Going deeper with convolutions. In *Proceedings of the IEEE Conference on Computer Vision and Pattern Recognition*, pages 1–9.

[Wang, 2016] Wang, Y.-Q. (2016). Small neural networks can denoise image textures well: a useful complement to bm3d. *Image Processing On Line*, 6:1–7.

[Williams and Hinton, 1986] Williams, D. and Hinton, G. (1986). Learning representations by back-propagating errors. *Nature*, 323:533–536.